

DIJET PRODUCTION IN PHOTON-PHOTON COLLISIONS AT $\sqrt{s_{ee}} = 161$ AND 172 GEV ^a

ROLAND BÜRGIN
for the OPAL collaboration
*Universität Freiburg, Hermann-Herder-Straße 3,
D-79104 Freiburg, Germany*

Dijet production is studied in collisions of quasi-real photons radiated by the LEP beams at e^+e^- centre-of-mass energies $\sqrt{s_{ee}} = 161$ and 172 GeV. Jets are reconstructed using a cone jet finding algorithm in the range $|\eta^{\text{jet}}| < 2$ and $E_T^{\text{jet}} > 3$ GeV. The angular distributions of direct and double-resolved processes and the inclusive two-jet cross-section are measured. They are compared to next-to-leading order perturbative QCD calculations and the prediction of the leading order Monte Carlo generators PYTHIA and PHOJET.

1 Introduction

The production of dijet events in the collision of two quasi-real photons is used to study the structure of the photon and different QCD predictions. The measurement of inclusive jet cross-sections and the comparison with next-to-leading order (NLO) QCD calculations and different photon structure functions can constrain the relatively unknown gluonic content of the photon.

2 Event selection and jet finding

To select a data sample of two-photon events the following set of cuts was applied. The sum of all energy deposits in the electromagnetic calorimeter (ECAL) and the hadronic calorimeter (HCAL) has to be less than 45 GeV. The visible invariant hadronic mass, W_{ECAL} , measured in the ECAL has to be greater than 3 GeV. The missing transverse energy of the event measured in the ECAL and the forward calorimeters has to be less than 5 GeV. At least 5 tracks must have been found in the tracking chambers. Events with detected scattered electrons (single-tagged or double-tagged events) are excluded from the analysis.

The results of the cone jet finding algorithm depend on the minimal transverse energy E_T^{min} and the cone size $R = \sqrt{(\Delta\eta)^2 + (\Delta\phi)^2}$ with the pseudorapidity $\eta = -\ln \tan(\theta/2)$ and the azimuthal angle ϕ . Here the values were chosen to be $R = 1$ and $E_T^{\text{min}} = 3$ GeV. The jet pseudorapidity in the laboratory frame is required to be within $|\eta^{\text{jet}}| < 2$.

^aTo be published in the proceedings of PHOTON'97, Egmond aan Zee

After applying all cuts and requiring at least two jets 2681 events remain in the data corresponding to an integrated luminosity of 20 pb^{-1} . For the simulation of two-photon interactions the Monte Carlo generators PYTHIA ¹ and PHOJET ² have been used. The mean Q^2 of the selected Monte Carlo events is 0.06 GeV^2 . About 1.2 % of the events in the data sample are expected to be e^+e^- annihilation events with hadronic final states and 0.2 % electron-photon events.

3 Angular distributions in direct and resolved events

A pair of variables, x_γ^+ and x_γ^- , can be defined which is related to the fraction of the photon energy participating in the hard scattering:

$$x_\gamma^+ = \frac{\sum_{\text{jets}=1,2} (E + p_z)}{\sum_{\text{hadrons}} (E + p_z)} \quad \text{and} \quad x_\gamma^- = \frac{\sum_{\text{jets}=1,2} (E - p_z)}{\sum_{\text{hadrons}} (E - p_z)}, \quad (1)$$

where p_z is the momentum component along the z axis of the detector and E is the energy of the jets or hadrons. If an event contains more than two jets, the two jets with the highest E_T^{jet} values are taken. Samples with large direct and double-resolved contributions can be separated by requiring both x_γ^+ and x_γ^- to be larger than 0.8 (denoted as $x_\gamma^\pm > 0.8$) or both values to be smaller than 0.8 (denoted as $x_\gamma^\pm < 0.8$), respectively ³.

The transverse energy flow around the jet axis for double-resolved events is expected to show additional activity outside the jet due to the photon remnants compared to the direct events. Figure 1 therefore shows the transverse energy flow around the jets with respect to the jet direction for data samples with different x_γ^\pm cuts. The pseudorapidity difference is defined by:

$$\Delta\eta' = k(\eta - \eta^{\text{jet}}).$$

The factor k is chosen event-by-event to be $k = +1$ for events with $x_\gamma^+ > x_\gamma^-$ and $k = -1$ for events with $x_\gamma^+ < x_\gamma^-$. Due to the definition of $\Delta\eta'$ there is always more of the remnant found at $\Delta\eta' < 0$ and the enhancement due to the additional transverse energy flow at negative and positive $\Delta\eta'$ is asymmetric. The jets in the data sample with $x_\gamma^\pm > 0.8$ are more collimated and there is almost no activity outside the jet whereas the transverse energy flow of two-jet events with $x_\gamma^\pm < 0.8$ shows additional activity outside the jets.

In the centre-of-mass system of the interacting partons or bare photons the parton scattering angle θ^* is defined as the angle between the jet axis of

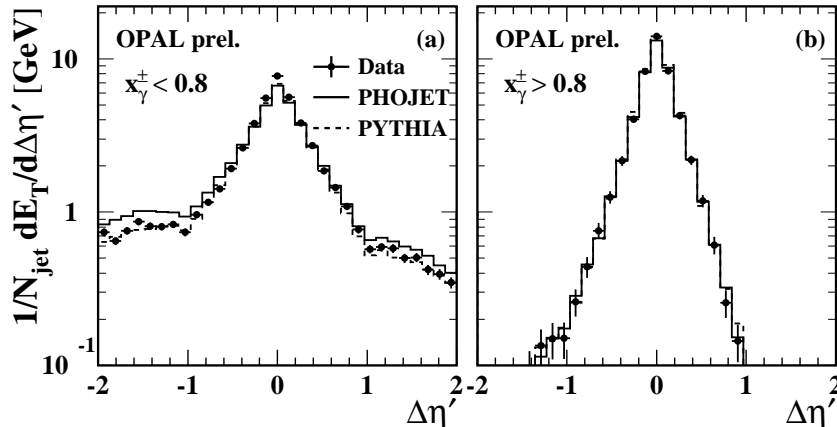


Figure 1: Uncorrected energy flow transverse to the beam direction measured relative to the direction of each jet in two-jet events. Jets from data samples with a large contribution of (a) double-resolved and (b) direct events according to their x_{γ}^+ and x_{γ}^- values are shown. The energy flow is integrated over $|\Delta\phi| < \pi/2$. Statistical errors only are shown.

the jets originating from the outgoing partons and the axis of the incoming partons or bare photons. The angular distribution of the jets can be used to check the separation between the different event classes using a variable which is not directly correlated to the definition of x_{γ}^+ and x_{γ}^- . In the dijet centre-of-mass frame one expects different angular distributions for direct and double-resolved events. An estimator of the angle between the jets and the parton-parton axis in the dijet centre-of-mass frame can be formed from their pseudorapidities. The variable $\cos\theta^*$ is calculated as

$$\cos\theta^* = \tanh\left(\frac{\eta^{\text{jet1}} - \eta^{\text{jet2}}}{2}\right).$$

Since the ordering of the jets is arbitrary, only $|\cos\theta^*|$ can be measured. The matrix elements of elastic parton-parton scattering processes have been calculated in LO⁴. The cut on E_T^{jet} restricts the accessible range of values of $|\cos\theta^*|$. Requiring the invariant mass of the dijet system to be larger than 12 GeV ensures that values of $|\cos\theta^*| < 0.85$ are not biased by the E_T^{jet} cut. The boost of the two-jet system in the z direction is defined by $\bar{\eta} = (\eta^{\text{jet1}} + \eta^{\text{jet2}})/2$. The detector resolution on $|\cos\theta^*|$ deteriorates significantly for events with $|\bar{\eta}|$ larger than 1. These events were therefore rejected by requiring $|\bar{\eta}| < 1$.

Figure 2 shows the $|\cos\theta^*|$ -distribution of events with $x_{\gamma}^{\pm} > 0.8$ and of events with $x_{\gamma}^{\pm} < 0.8$. The dependence on the Monte Carlo models used

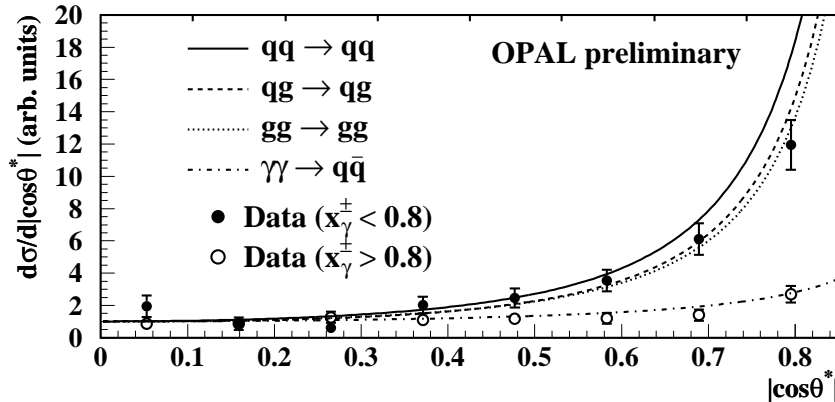


Figure 2: Angular distribution of events with large direct and large double-resolved contributions according to the separation with x_γ^+ and x_γ^- . The data are compared to QCD matrix element calculations⁴. The data are normalised to have an average value of 1 in the first three bins and the curves are normalised to be 1 at $\cos(0)$.

is taken into account by adding the difference between the results obtained with PYTHIA, which are taken to be the central values, and PHOJET to the systematic error. The error bars show the statistical and the systematic errors added in quadrature. The events with $x_\gamma^\pm > 0.8$ show a small rise with $|\cos\theta^*|$, whereas the events with $x_\gamma^\pm < 0.8$ show a much stronger rise in $|\cos\theta^*|$. The data points of the events with $x_\gamma^\pm < 0.8$ are compared with the prediction of a QCD matrix element calculation of the interaction of quarks or gluons in the photon. The matrix elements with a relevant contribution to the cross-section where antiquarks are involved instead of quarks show a similar behaviour as the examples shown. The QCD matrix element calculations agree well with the data points of the data samples with large direct and large double-resolved contribution.

4 Inclusive two-jet cross-sections

The inclusive two-jet cross-section is measured using a cone jet finding algorithm with a cone size $R = 1$. The data were corrected for the selection cuts, the resolution effects of the detector and the background from non-signal processes. In Fig. 3, the inclusive two-jet cross-section is shown as a function of E_T^{jet} . The bin sizes, which are indicated by the vertical lines at the top of the figure, approximately reflect the experimental resolution.

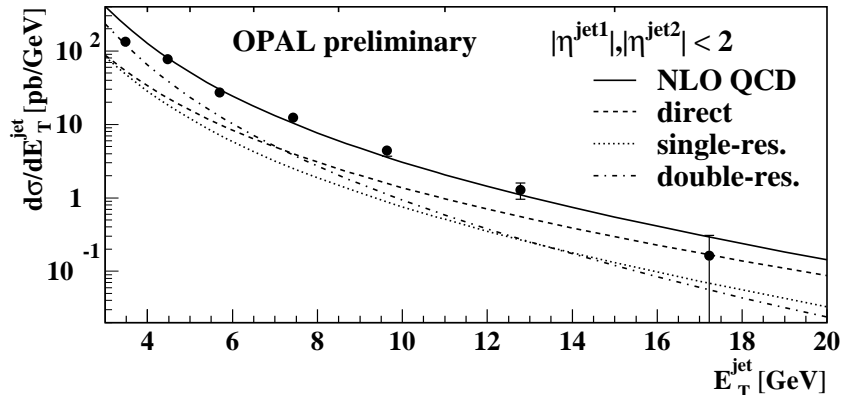


Figure 3: The inclusive two-jet cross-section as a function of E_T^{jet} for jets with $|\eta^{\text{jet}}| < 2$ compared to the NLO calculation by Kleinwort and Kramer⁵. The direct, single-resolved and double-resolved cross-sections and the sum (continuous line) are shown separately.

The E_T^{jet} distribution is compared to an NLO perturbative QCD calculation of the inclusive two-jet cross-section by Kleinwort and Kramer⁵ who use the NLO GRV parametrisation of the photon structure function⁶. Their calculation was repeated for the kinematic conditions of this analysis. The direct, single- and double-resolved parts and their sum are shown separately. The resolved cross-sections dominate in the region $E_T^{\text{jet}} \lesssim 8$ GeV, whereas, at high E_T^{jet} the direct cross-section is largest. The data points are in good agreement with the calculation except in the first bin where the NLO calculation is not reliable due to IR singularities. The uncertainties due to the modelling of the hadronisation process are expected to contribute mainly at low E_T^{jet} values.

The inclusive two-jet cross-section, which is dominated by the low E_T^{jet} events, depends on the parton density function of the photon which mainly differs in the assumptions on the gluon part of the photon. In 40 to 60 % of all processes at least one gluon from the photon interacts depending on the parton density function used. This leads to different predictions of the inclusive two-jet cross-section. The inclusive two-jet cross-section as a function of $|\eta^{\text{jet}}|$ is shown in Fig. 4. The inclusive two-jet cross-section predicted by the two Monte Carlo models differ significantly even if the same photon structure function is used. This model dependence currently reduces the sensitivity to the parametrisation of the photon structure function. The GRV-LO and SaS-1D parametrisations^{6,7} describe the data equally well, but the LAC1 parametrisation⁸ overestimates the inclusive two-jet cross-section significantly.

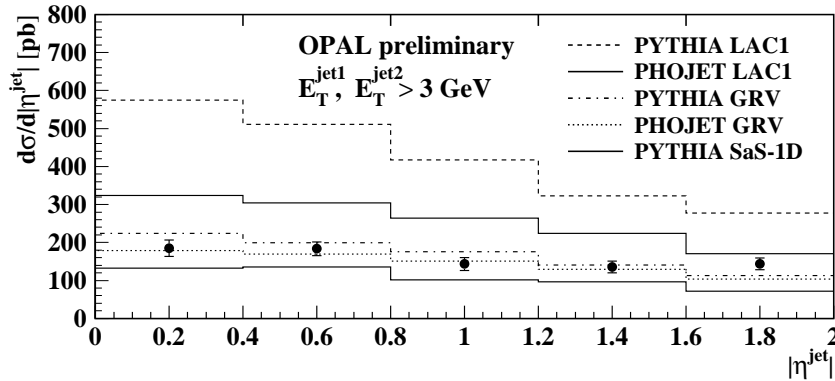


Figure 4: The inclusive two-jet cross-section as a function of $|\eta^{\text{jet}}|$ for jets with $E_T^{\text{jet}} > 3$ GeV.

5 Conclusions

The distribution of the parton scattering angle θ^* of data samples with large direct and double-resolved contributions separated experimentally using the variables x_γ^+ and x_γ^- have been compared to the relevant QCD matrix element calculations. The inclusive two-jet cross-sections were measured as a function of E_T^{jet} and $|\eta^{\text{jet}}|$. The E_T^{jet} dependent two-jet cross-section is in good agreement with an NLO QCD calculation. The GRV-LO and SaS-1D parametrisations describe the inclusive two-jet cross-section equally well. The LAC1 parametrisation overestimates the inclusive two-jet cross-section significantly.

1. T. Sjöstrand, Comp. Phys. Commun. 82 (1994) 74; T. Sjöstrand, LUND University Report, LU-TP-95-20 (1995).
2. R. Engel and J. Ranft, Phys. Rev. D54 (1996) 4244; R. Engel, Z. Phys. C66 (1995) 203.
3. OPAL Collaboration, K. Ackerstaff et al., Z. Phys. C73 (1997) 433.
4. B. L. Combridge et al., Phys. Lett. B70 (1977) 234; D. W. Duke and J. F. Owens, Phys. Rev. D26 (1982) 1600.
5. T. Kleinwort, G. Kramer, DESY-96-035 (1996); T. Kleinwort, G. Kramer, Phys. Lett. B370 (1996) 141.
6. M. Glück, E. Reya and A. Vogt, Phys. Rev. D46 (1992) 1973; M. Glück, E. Reya and A. Vogt, Phys. Rev. D45 (1992) 3986.
7. G. A. Schuler and T. Sjöstrand, Z. Phys. C68 (1995) 607.
8. H. Abramowicz, K. Charchula and A. Levy, Phys. Lett. B269 (1991) 458.